Dalton Transactions

Accepted Manuscript

ROYAL SOCIETY OF CHEMISTRY

www.rsc.org/dalton

Dalton Transactions

ARTICLE

Versatility of the Ionic Assembling Method to Design Highly Luminescent PMMA Nanocomposites Containing $[M_6Q^i_8L^a_6]^{n-}$ Octahedral Nano-building Blocks

Received 00th January 20xx,
Accepted 00th January 20xx

DOI: 10.1039/x0xx00000x

www.rsc.org/

Maria Amela-Cortes,*[a, b] Yann Molard,*[a] Serge Paofai,[a] Anthony Desert,[c] Jean-Luc Duvail,[c] Nikolay G. Naumov[d] and Stéphane Cordier[a]

New luminescent poly(methylmethacrylate) (PMMA) nanocomposites with high content of different hexanuclear octahedral cluster building blocks, namely $[Mo_6I_8(C_2F_5COO_6)]^{2-}$, $[Re_6Se_8(CN)_6]^{4-}$ and $[W_6Cl_{14}]^{2-}$ have been prepared by free-radical polymerisation. To do so, cluster complexes bearing a polymerisable ammonium counter-cation have been synthesised. In this way, we demonstrate that ionic assembling is a powerful tool to functionalise easily any type of anionic cluster units to be introduced in a PMMA organic matrix. All samples remain homogeneous, stable during several months, and keep the luminescence properties of the cluster precursor.

Introduction

Incorporation of inorganic nanoparticles into polymers has become an important strategy for improving functionalities of materials. One can combine in a unique material the specific functionalities of inorganic components, such as magnetic or optical properties, to the ease of processability, adaptability and low cost of organic polymers.[1] In particular, photoluminescent hybrid materials that merge inorganic dyes with a polymer matrix are promising materials for applications related to photonics, optoelectronics and lighting compared to conventional organic dyes containing material, because of their higher photostability.[2] Examples of nanometric dyes that have been incorporated into polymer matrices are ZnO nanocrystals,[3] quantum dots,[4] polyoxometalates[5-8] or gold nanoparticles.[9] One of the major challenges is to obtain homogeneous highly doped hybrid polymers in order to enhance the photoluminescence properties as well as the thermal stability of the material, while maintaining a good processability. $A_n[M_6Q^i_8X^a_6]$ (A = alkali; M = Mo, Re, W; Q = chalcogen/halogen, X = halogen) octahedral transition metal cluster compounds, obtained via high temperature synthesis, are an attractive class of molecular inorganic nanomaterials to develop nanocomposites. They have been introduced into liquid crystalline materials,[10, 11] supramolecular architectures,[12, 13] polymeric frameworks[14] or nanomaterials.[12, 15, 16] $[M_6Q^i_8X^a_6]^{n-}$ (n = 2, 3 or 4) units are characterized by a rigid $(M_6Q^i_8)^{m+}$ cluster core (m = 4, 3 or 2) with interesting structural, electronic and photochemical properties related to the number of metallic electrons available for metal-metal bonds (VEC).[17, 18] Among these properties, they are highly emissive in the red-NIR region with lifetimes in the range of several tenths of microseconds and photoluminescence quantum yields up to 1.[19, 20] Within the solid, the charge balance of discrete $[M_6Q^i_8X^a_6]^{n-}$ units is generally assumed by alkali or divalent cations. The ceramic-like behaviour (brittle and low plasticity) in the solid state of such inorganic phosphors strongly limits their direct incorporation into polymeric matrices, since usually it leads to phase segregation between the inorganic and organic parts.[5, 21] Therefore, new strategies to integrate them in optical devices need to be explored. Many studies have been focused in the last decades on the solubilisation of inorganic clusters in aqueous and organic media.[22, 23] Some examples exist in the literature where octahedral clusters, mainly Mo_6 clusters, have been incorporated into polymers. The usual methodology consists in the grafting of six polymerisable units in apical positions of the inorganic cluster core. The first example was described by Golden *et al.*[24] where inorganic Mo_6 clusters were introduced in a polymer host by using a "monomer as a solvent" method. To do so, they substituted the six weakly bound apical triflate ligands of $[Mo_6Cl_8(OTf)_6]^{2-}$ with N-vinylimidazole (NVI) moieties.

[a] Institut des Sciences Chimiques de Rennes, UR1-CNRS 6226, Groupe Chimie du Solide et Matériaux, Université de Rennes 1, Campus Beaulieu, CS 74205, 35042 Rennes Cedex (France). maria.amela-cortes@univ-rennes1.fr, yann.molard@univ-rennes1.fr
[b] SATT Ouest-Valorisation, 14C Rue du Pâtis Tatelin, Metropolis 2, CS 80 804, 35708, Rennes Cedex (France).
[c] Institut des Matériaux Jean Rouxel, CNRS, IMN, UMR 6502 CNRS-Université de Nantes, F-44322 Nantes (France).
[d] Nikolaev Institute of Inorganic Chemistry, Siberian Branch of the Russian Academy of Sciences, 3 Acad. Lavrentiev pr., 630090 Novosibirsk (Russia), Novosibirsk State University, 3, Pirogova str., 630090 Novosibirsk (Russia)

Electronic Supplementary Information (ESI) available: ^{19}F and ^{1}H NMR spectra of clusters and polymers, pictures of PMMo1, PMRe1 and PMW1 under daylight, SEM and TEM images of PMMo50, PMRe20 and PMW50, DSC traces of PMMox, TGA thermograms of PMMox, PMRe1, PMRe20, PMW1 and PMW50; luminescence spectra of polymerisable clusters and PMRE1, PMRE20, PMW1 and PMW50. See DOI: 10.1039/x0xx00000x

After substitution, the functionalised cluster was dispersed in NVI monomer and copolymerised. By this method, highly crosslinked, swellable polymers where obtained. Surprisingly, the luminescence properties of the final hybrid polymer were not reported. The same approach was used by Adamenko *et al.*[25] by replacing some of the six trifluoroacetate ligands of $[Mo_6Cl_8(CF_3COO)_6]^{2-}$ with acrylate moieties to obtain $[Mo_6Cl_8(CF_3COO)_{6-n}(CH_2{=}CHCOO)_n]^{2-}$ (n = 1-3) which was copolymerised with methacrylic acid. In this case, the cluster luminescence properties were lost after ageing. Robinson *et al*.[26] also found highly cross-linked polymers by introducing $[Mo_6Cl_8(OTf)_6]^{2-}$ and $[Mo_6Cl^i{}_8Cl^a{}_4(EtOH)_2]$ into polyvinylpyridine. After the polymerisation, the luminescence of the triflate cluster unit was quenched while, for the second one, the luminescence properties were maintained. We recently used this approach in which the six fluorine atoms in apical position of $[Mo_6Br_8F_6]^{2-}$ were substituted by methacrylic moieties to afford $[Mo_6Br_8(CH_2{=}C(CH_3)COO)_6]^{2-}$. Afterwards, it was copolymerised within a methylmethacrylate monomer solution.[27] Even though the luminescence properties of the cluster core were maintained in the polymer, the cluster could not be introduced in high content, (more than 0.36 wt %) because of its high crosslinking density. Only few examples dealing with the introduction of Re_6 and W_6 clusters into polymers are found in the literature. Zheng *et al.* have introduced monofunctionalised Re_6 clusters with vinylpyridine, in the side chain of polystyrene strands, by copolymerisation.[28] The same team also introduced Re_6 clusters by Atom Transfer Radical Polymerisation to form non-cross-linked poly(methylmethacrylate) (PMMA) hybrids.[29] However, the luminescence properties of the hybrid were not reported. We have previously incorporated bifunctional Re_6 clusters, $[Re_6Se_8(TBP)_4(MAC)_2]$ (TBP = p-tert-butylpyridine; MAC = methacrylic acid) into a PMMA matrix by using bulk and solution polymerisation.[30] We showed that the luminescence properties of the cluster core were retained in the final polymer. Following the same principle, Efremova *et al.* introduced up to 10 wt% of Re_6 cluster, trans-$[Re_6Q_8(TBP)_4(VB)_2]$ where Q = S, Se; VB = vinylbenzoate), by solution polymerisation in chlorobenzene.[31] In their case also the cluster luminescence properties were retained. The lack of a general method to introduce the clusters into a polymeric matrix prompted us to develop a new approach that allows their integration at high content into a PMMA matrix.[32] The method has been previously described for the incorporation of anionic polyoxometalates into PMMA and polystyrene matrices through electrostatic interactions.[7, 8, 33, 34] Using this approach, we have successfully introduced up to 50 wt% of $[Mo_6Br^i{}_8Br^a{}_6]^{2-}$ cluster units functionalised by ammonium cations bearing a polymerisable group in terminal position. In this study, we aim to demonstrate the versatility of the method by doping a PMMA matrix with octahedral anionic cluster units containing different types of metal atoms and/or bearing different charges, namely: $[Mo_6I_8(C_2F_5COO)_6]^{2-}$, $[W_6Cl_{14}]^{2-}$ and $[Re_6Se_8(CN)_6]^{4-}$. Note that for $[Re_6Se_8(CN)_6]^{4-}$, bearing a 4- charge, four polymerisable ammonium cations per octahedral metallic unit are introduced instead of only two when $[Mo_6I_8(C_2F_5COO)_6]^{2-}$ or $[W_6Cl_{14}]^{2-}$ are functionalised. Thus the Re_6 cluster unit, paired with four ammonium cations, could be seen as a stronger cross-linker although we prove that we can still introduce a high content of it in the polymer, compared to previous works described above. The fact that the polymerisable moiety is included on the counter-cation unit allows the easy functionalisation of any type of cluster presenting an anionic character without modifying the apical ligand around the cluster core. This allows to maintain the cluster core intact and thus, its intrinsic optical properties. The clusters have been integrated in different ratio into the PMMA matrix and the thermal and optical properties have been studied. Moreover, we show for the first time, highly emissive hybrid polymers based on octahedral Mo_6 clusters as well as the first W_6-PMMA nanocomposite obtained by bulk polymerisation.

Experimental Section

Starting materials were purchased from Aldrich or Alfa Aesar. Methyl methacrylate was distilled before use. Azobisisobutyronitrile (AIBN) was recrystallized from ether. The polymerisable organic ammonium salt (KatPBr) was prepared following a reported procedure.[32] The clusters precursors were synthesised according to reported procedures: $(H_3O)_2W_6Cl_{14}(H_2O)_7$ [35] (**2**), $K_4Re_6Se_8(CN)_6$ (**3**),[36] and $Cs_2Mo_6I_{14}$[22]. NMR experiments were realized on a Bruker Ascend 400 MHz NMR spectrometer. Elemental analysis was performed with a Flash EA1112 microanalyzer in Centre Régional de Mesures Physiques de l'Ouest (CRMPO).

$Cs_2Mo_6I_8(C_2F_5COO)_6$ (**1**): To a solution of $Cs_2Mo_6I_{14}$ (1.5 g, 0.52 mmol) in 20 mL of acetone, was added a solution of silver pentafluoropropionate (0.935 g, 3.42 mmol) in 10 mL of acetone under argon and in the dark. The mixture was stirred for 48 h in the dark and then was filtered through a Celite® pad. The red solution was then evaporated to yield a red-orange powder.^{19}F-NMR (acetone-d_6): δ (ppm) = -83 (3F), -120 (2F). EDAX: Cs 2, Mo 8, I 11, F 77, no Ag.

Structural data of $Cs_2Mo_6I_8(C_2F_5COO)_6$ - 2 $C_4H_{10}O$. Further details on the crystal-structure investigations may be obtained from the Cambridge Crystallographic Data Centre (CCDC 1427095) or from the FIZ Karlsruhe, Germany, (CSD-429127). Formula:$C_{26}Cs_2I_8Mo_6O_{14}H_{20}$, sample size = 0.54 × 0.4 × 0.23 mm^3, λ = 0.71069 Å (Mo Kα), Bruker AXS APEX-II diffractometer, T = 150(2), triclinic system, space group *P*-1 (N° 2), Mr = 2983.08 g mol^{-1}, ρ_{calc} = 3.079 g cm^3, a = 10.3047(5) Å, b = 12.9000(6) Å, c = 13.2277(6) Å, α = 113.660(2), β = 92.194(2), γ = 90.476(3), V = 1608.84(13) Å^3 , Z = 1, multiscan absorption correction (SADABS), SHELXL-2014, 7390 independent reflections, 378 parameters, (Sheldrick, 2014), R_1 = 0.0402 [I > 2 σ (I)], wR_2 = 0.0942, GooF = 1.165, largest difference peak and hole +2.60 and -2.53 e·Å^{-3}. Important interatomic distances range within $[Mo_6I_8(C_2F_5OCO)_6]^{2-}$ cluster units (Å): Mo-Mo: 2.6586(5)-2.6674(7); Mo1-I: 2.7646(6)-2.7889(6); Mo-O: 2.127(4)-2.149(4). Single crystals were obtained in few hours after adding aliquots of diethylether directly on the acetone wetted powdered sample.

(KatP)$_2$[Mo$_6$I$_8$(C$_2$F$_5$COO)$_6$] (**4**): $Cs_2[Mo_6I_8(C_2F_5OCO)_6]$ (0.72 g, 0.25 mmol) was solubilised in a minimum of dry acetone. To that a solution of KatPBr (0.23 g, 0.5 mmol) in acetone (10 ml) was added dropwise. A white precipitate of CsBr formed instantaneously. The mixture was left for 1 h at room temperature. The mixture was filtered through a Celite pad and the solvent was removed under vacuum. The obtained powder was further solubilized in CH_2Cl_2, the solution was filtered through a microfilter to remove any remaining CsBr and evaporated to yield compound (**4**) as a red-orange oil. Yield 97%.^{1}H-NMR (400 MHz, acetone-d^6): δ (ppm) = 6.06 (d, 2H, CHH=C), 5.62 (d, 2H, CHH=C), 4.13 (t, 4H, -CH$_2$-O), 3.53 (t, 8H, -CH$_2$-N), 3.33 (s, 12H, CH$_3$N-), 1.92 (s, 6H,-CH$_3$-C), 1.66 (m, 4H,-(CH$_2$-CH$_2$)O), 1.42-1.29 (m, 72H, -CH$_2$-), 0.89 (t, 6H, -CH$_3$). ^{19}F-NMR (acetone-d^6): δ (ppm) = -83 (3F), -120 (2F). Elemental analysis $C_{76}H_{116}N_2O_{16}F_{30}I_8Mo_6.3CH_2Cl_2$: calc (%): C 25.50, H 3.09, N 0.75. Found: C 25.54, H 3.25, N 0.73.

(KatP)$_2$[W$_6$Cl$_{14}$] (**5**): $(H_3O)_2W_6Cl_{14}(H_2O)_7$ (0.38 g, 0.23 mmol) was dissolved in 5 mL of absolute EtOH. A solution of KatPBr (0.21 g, 0.5 mmol) in 10 mL of dichloromethane was added dropwise to the cluster solution. The mixture was heated for 1 hour and the solvents evaporated under vacuum. The residue was dissolved in the minimum amount of acetone and filtered through a Celite® pad. The acetone was removed under vacuum. The obtained crude mixture was further solubilized in CH_2Cl_2, the solution was filtered through a microfilter to remove any remaining solid and evaporated to yield compound (**5**) that was obtained as a yellow oil. Yield 95%.^{1}H-NMR (400 MHz, CD_2Cl_2): δ (ppm) = 5.97 (d, 2H, C<u>H</u>H=C), 5.48 (d, 2H, C<u>H</u>H=C), 4.03 (t, 4H, -CH$_2$-O), 3.15 (t, 8H, -CH$_2$-N), 3.01 (s, 12H, CH$_3$N-), 1.84 (s, 6H,-CH$_3$-C), 1.7 – 1.60 (m, 8H,-(C<u>H$_2$</u>-CH$_2$)$_2$N), 1.59 (m, 4H,-C<u>H$_2$</u>-CH$_2$-O), 1.31 – 1.20 (m, 64H, -CH$_2$-), 0.80 (t, 6H, -CH$_3$). ^{13}C-NMR (400 MHz, CD_2Cl_2): 167.5 (C=O), 136.7 (C(Me)=CH$_2$), 124.9 (CH$_2$=C), 65.1 (CH$_2$O), 64.83 (CH$_2$N), 51.9 (CH$_3$N),31.9-22.7 (CH$_2$), 18.1 (CH$_3$ (C=CH$_2$), 13.9 (CH$_3$). Elemental analysis $C_{58}H_{116}N_2O_4Cl_{14}W_6.6CH_2Cl_2$: calc (%): C 25.50, H 4.28, N 0.93. Found: C 25.32, H 4.24, N 1.04.

(KatP)$_4$[Re$_6$Se$_8$(CN)$_6$] (**6**): $K_4Re_6Se_8(CN)_6$ $3.5H_2O$ (0.4 g, 0.19 mmol) was solubilised in 5 mL of distilled water. A solution of KatPBr (0.35 g, 0.77 mmol) in 5 ml of dichloromethane was added dropwise to the stirred water solution. The biphasic mixture was vigorously stirred for 1 h. After that the phases were allowed to separate and the organic phase was collected and washed three times with water. The dichloromethane was removed under vacuum to afford compound 6 as a dark red solid. Yield 95%.^{1}H-NMR (400 MHz, CD_2Cl_2): δ (ppm) = 5.98 (d, 4H, C<u>H</u>H=C), 5.46 (d, 4H, C<u>H</u>H=C), 4.03 (t, 8H, -CH$_2$-O), 3.19 (m, 20H, -CH$_2$-N+CH$_3$-N), 1.84 (s, 12H,-CH$_3$-C), 1.7 – 1.60 (m, 16H,-(C<u>H$_2$</u>-CH$_2$)$_2$N), 1.59 (m, 8H,-C<u>H$_2$</u>-CH$_2$-O), 1.31 – 1.20 (m, 128H, -CH$_2$-), 0.80 (t, 12H, -CH$_3$). ^{13}C-NMR (400 MHz, CD_2Cl_2): 167.5 (C=O), 136.7 (C(Me)=CH$_2$), 124.6 (CH$_2$=C), 64.7 (CH$_2$O), 64.0 (CH$_2$N), 52.7(CH$_3$N), 31.9-22.7 (CH$_2$), 18.1 (CH$_3$ (C=CH$_2$), 13.9 (CH$_3$). EDAX: no potassium, no bromide; Re 47.45%, Se 47.34. Elemental analysis $C_{122}H_{232}N_{10}O_8Se_8Re_6.2CH_2Cl_2$: calc (%): C 38.33, H 6.12, N 3.60. Found: C 38.25, H 6.21, N 3.79.

Polymerisation: The corresponding polymerisable cluster was dissolved in freshly distilled methylmethacrylate: Mo$_6$: from 1 wt% to 50 wt%; W$_6$: 1 wt% and 50 wt%; Re$_6$: 1 wt% and 20 wt%. After addition of 0.2 wt% of the radical initiator AIBN, the solutions were sonicated for 5 min to obtain homogeneous solutions. For W$_6$ and Re$_6$ clusters, two drops of acetonitrile were added to help the solubilisation of clusters. The solutions were heated in an oil-bath at 81 °C for 2 h. The viscous pre-polymers were then placed in an oven at 60 °C for 24 h and then annealed at 100 °C for 4 h. For sake of clarity, composite will be named in the following as: PMYx with Y= Mo, W or Re when (**4**), (**5**) or (**6**) were introduced respectively, and with x = the weight percentage of (**4**), (**5**) or (**6**) within the material. Transparent pellets were obtained unless for the hybrid containing 20 wt% of Re$_6$ cluster (PMRe20). ^{1}H-NMR spectra of dissolved pellets (except for PMW50, which is only partially soluble) are provided in the ESI (Fig S2, S3, S4).

Transmission electron microscopy (TEM): TEM characterizations were performed using a Hitachi HF-2000 operating at 100 kV and equipped with a cryo holder. For PMMo50 and PMW50, layers of 100 nm were cut in the pellet by ultramicrotomy and deposited on TEM copper grids covered with a thin holey carbon film. For PMRe20, the composite was dissolved in chloroform and then deposited on a TEM copper grid covered with a thin silica film.

Scanning electron microscopy (SEM): SEM characterizations were performed using a JEOL JSM-7600F operating at 5-15 kV. Sections of the PMMo50, PMRe20 and PMW50 pellets were deposited on silicon substrate and Pt-metalized.

Thermal analysis: DSC measurements were realized at 10 K min^{-1} with a DSC 200 F3 Maia NETSCH apparatus. Thermogravimetric analysis were realized at 10 K min $^{-1}$ on a TGA/DT Perkin Pyris Diamond.

Size exclusion chromatography (SEC analysis): SEC analysis were performed using a set of three columns: 2xResiPore and 1x PL gel Mixed C (Polymer Labs.). The detection system was composed of a refractometer and a UV detector. Chloroform was used as eluent with a flow rate of 0.8 mL min^{-1}. The elution profiles were analysed by software Empower GPC module (Waters). Calculations were based on calibration curves obtained from polystyrene standards ranging from 200 g mol^{-1} up to 6 x 10^6 g mol^{-1}. For the analysis, samples were refluxed 30 min in chloroform. The obtained solutions were filtered prior injection.

Spectroscopic characterisation: Photostability experiments and luminescence measurements were recorded with an Ocean Optics QE6500 CCD spectrophotometer by irradiating the samples with a Nikon-intensilight C-HGFI (UV 1 filter, 350 nm < λ_{exc} < 380 nm). Spectra are given in relative irradiance to take into account the nonlinear answer of the set-up sensitivity (an Ocean Optics HL-2000-CAL Calibrated Tungsten Halogen Light Source was used to calibrate the all set-up). Absolute quantum yield were measured with a Hamamatsu C9920-03G system.

Results and Discussion

Synthesis strategy.

Three different cluster units have been used for the study namely, $[Mo_6I_8(C_2F_5COO)_6]^{2-}$, $[W_6Cl_{14}]^{2-}$ and $[Re_6Se_8(CN)_6]^{4-}$. They were prepared as $Cs_2[Mo_6I_8(C_2F_5COO)_6]$ (**1**), $(H_3O)_2[W_6Cl_{14}]$ (**2**) and $K_4[Re_6Se_8(CN)_6]$ (**3**) salts, respectively. Compound (**1**), bearing pentafluoropropionate groups in apical position, was chosen because of the high quantum yields recently reported by Sokolov *et al.*[19] and Kirakci *et al.*[20] for similar clusters functionalised by fluorinated carboxylate ligands. Indeed, quantum yields of 0.59 and 1 were reported in solution for $(n\text{Bu}_4\text{N})_2\text{Mo}_6\text{I}_8(n\text{-}C_3F_7CO_2)_6$ and $(n\text{Bu}_4\text{N})_2\text{Mo}_6\text{I}_8(CF_3CO_2)_6$, respectively. In compound (**1**), the anionic cluster unit is associated to a Cs^+ counter-cation. Indeed, an alkali counter-cation is mandatory to functionalise the anionic cluster unit with polymerisable ammonium cations by a metathesis reaction. $Cs_2Mo_6I_8(C_2F_5OCO)_6$ was prepared from $Cs_2Mo_6I^i{}_8I^a{}_6$ and $AgOCOC_2F_5$. The integrity and purity of the compound was confirmed by ^{19}F-NMR with the presence of only two signals at δ = -83 ppm and δ = -120 ppm (ESI, fig S1), by EDAX and by X-ray diffraction on single crystals (see **Figure 1** and experimental part for details about the crystal structure). Compound (**2**) was prepared by a reported procedure,[35] so as compound (**3**).[36] In this last case, cyano groups in apical position were chosen instead of halogen or hydroxo groups to keep the integrity of cluster units during the cationic metathesis process.[37]

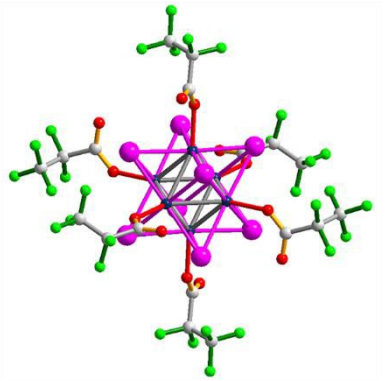

Figure 1. Representation according to single crystal data X-ray diffraction measurements of $Cs_2Mo_6I_8(C_2F_5OCO)_6$.

The functional clusters (**Scheme 1**) are obtained by a metathesis reaction between an ammonium cation containing two long alkyl chains from which one is functionalised with a methacrylate group in terminal position, and the cesium, hydronium or potassium cation, depending on the cluster complex.[10, 32] A similar polymerisable cation was previously used by Wu *et al*. to encapsulate polyoxometalates which were introduced by copolymerisation into PMMA or polystyrene latex.[8, 34] The polymerisable compound containing the Mo_6-based cluster (**4**) was obtained as a bright red oil, the one of W_6 (**5**) was a yellow solid and that of Re_6 (**6**) was a dark red solid. The identity and purity of the three polymerisable clusters was assessed by ^{1}H NMR, EDAX, elemental analysis and also by ^{19}F NMR for (**4**).

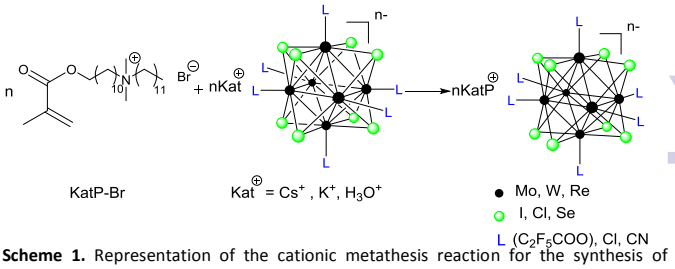

Scheme 1. Representation of the cationic metathesis reaction for the synthesis of functional clusters.

Synthesis and characterisations of PMMA-cluster doped nanocomposites.

PMMA was chosen to prepare the cluster nanocomposites for its excellent optical properties (i.e. transparency from the near UV to the near IR regions and damage resistance in the range needed for optical applications), thermal stability and easy shaping. To form the nanocomposites, functional cluster-based compounds were copolymerised in the bulk with neat MMA using azobisisobutyronitrile (AIBN) as initiator. The polymerisation was conducted first at 80 °C in an oil bath to form a pre-polymer for 2 hours and then the composites were placed in an oven and heated at 60 °C for 24h. The samples were then annealed at 100 °C for 4 hours. The ^{1}H NMR spectra of nanocomposites (see ESI, figure S2-S4) showed that a full conversion had occurred with the disappearance of doublets located between 6.0 and 5.5 ppm relative to the methylenic protons of the monomer double bond and the singlet at 1.90 ppm corresponding to the methyl protons of the methacrylic unit. Copolymers in form of pellets in 1, 10, 20 and 50 wt% content of (**4**) were obtained directly as the functional cluster was very soluble in MMA, whereas few drops of acetonitrile were necessary to allow the full solubilisation of (**5**) and (**6**) in the monomer. For (**6**), a maximum amount of 20 wt% could be introduced in the polymer. For higher ratio, the obtained composites became insoluble due to the higher cross-linking ability of the Re_6 tetra anionic cluster compared to the dianionic ones. The composites obtained with dianionic cluster units (**4**) and (**5**) were fully homogeneous showing high transparency up to 50 wt%. At this stage, we wish to stress that, in the following parts, all hybrid polymer samples will be named as described in the experimental section (polymerisation section). **Figure 2** shows digital images taken under daylight and under UV irradiation at 365 nm for PMMo10, PMMo20 and PMMo50 (ESI figure S5 for digital picture of pellets containing (**5**) or (**6**)). As the clusters are incorporated by electrostatic interactions, their cross-linking ability is limited. Hence, it allows their homogeneous dispersion even at high content and provides to the nanocomposites a good solubility in organic solvents. All PMMo samples were fully soluble in organic solvents such as chloroform and dichloromethane. This feature differs from the behaviour we recently encountered when copolymers were made of $[Mo_6Br_{14}]^{2-}$ cluster units, which were already partially insoluble at 20 wt%.[32] Possibly, the fluorinated ligands located in apical position in (**4**) impart additional mobility to the polymer chains. This is corroborated by the high molecular

weight found by GPC, which infers that the good solubility cannot be due to the formation of low molecular weight polymers, like when polymers are obtained by solution polymerisation, which would solubilise more readily.[11, 31] On the contrary, PMW50 was partially insoluble. PMRe20 copolymer was completely soluble albeit the four polymerisable groups present in the Re_6-based building block. All obtained pellets were optically transparent giving a good indication of the homogeneous distribution of the inorganic content in the PMMA copolymer matrix.

Figure 2. Digital photographs of the pellets PMMo10, PMMo20 and PMMo50 under visible (above) and under UV (λ_{exc} = 365 nm)

Transmission electron microscopy (TEM) and scanning electron microscopy (SEM) experiments were realized on the most concentrated samples i.e. PMMo50, PMW50 and PMRe20. The low contrast observed on the micrographs confirms the non-segregation of the inorganic components within the organic matrix and thus the homogeneous distribution of cluster units within the copolymers at the micro- and nanometric scale (ESI Fig. S6-S7). These results are in good accordance with our previous report dealing with the introduction at high content of $[Mo_6Br_{14}]^{2-}$ in PMMA. [32]

The composites thermal behaviour studied by DSC (**Table 1**, see ESI figure S8) evidenced that the T_g decreases as the content of (**4**) or (**5**) increases from 107 °C for neat PMMA to 83 or 90 °C for PMMo50 or PMW50, respectively. This could be attributed to the mobility of the ammonium head around the cluster core unit and to the flexibility of the alkyl chains. The fact that the T_g of PMMox is lower than that of PMWx can be attributed to the additional mobility that the pentafluoropropionate groups impart to the polymer. Surprisingly, PMRex samples do not follow this trend as the two samples show a T_g around 100 °C. The T_g for PMRe1 is lower than those of PMMo1 and PMW1 as the functional Re_6 cluster building block contains four ammonium heads with flexible alkyl chains.

The nanocomposites thermal stability was studied by TGA. The main weight loss step is located at 370 °C for pure PMMA and the introduction of inorganic clusters leads to an enhancement of the thermal stability of the material (Table 1. See ESI figure S9-S11). Nevertheless, the thermograms are different for all three types of copolymers. PMMo sample thermograms present a first step of weight loss occuring at 250 °C corresponding to the loss of the six pentafluoropropionate in apical position. In the case of PMRe, the first step corresponding to the loss of the six cyano groups in apical position is located at 311 °C. For PMW samples the decomposition occurs only in one step.

Table 1. Molecular weight from GPC measurements and thermal data of synthesised hybrid polymers

Sample	M_w (g mol^{-1})	T_g(°C)	T_d (°C)
PMMo0	366000	107	370
PMMo1	113000	107	407
PMMo10	130000	100	404
PMMo20	165000	92	399
PMMo50	128000	83	372
PMW1	558000	108	403
PMW50	---	90	402
PMRe1	627000	98	383
PMRe20	562000	99	394

Photophysical studies.

Photoluminescence properties were investigated on solid nanocomposite samples and compared to the one of their parent cluster precursor (ESI figure S12). **Figure 3a** shows the PMMo1, PMRe1 and PMW1 samples under UV irradiation at 365 nm. In a first attempt, it seems straightforward that PMMo samples are highly emissive in the red region compared to PMRe and PMW samples. The normalized emission spectra for the three hybrid polymers are depicted in **Figure 3b**. All samples emit red phosphorescence upon excitation anywhere in their absorption band (λ = 300-550nm). The clusters and corresponding nanocomposites show the same broad and structureless emission band between 550 and 950 nm typical of the cluster core.

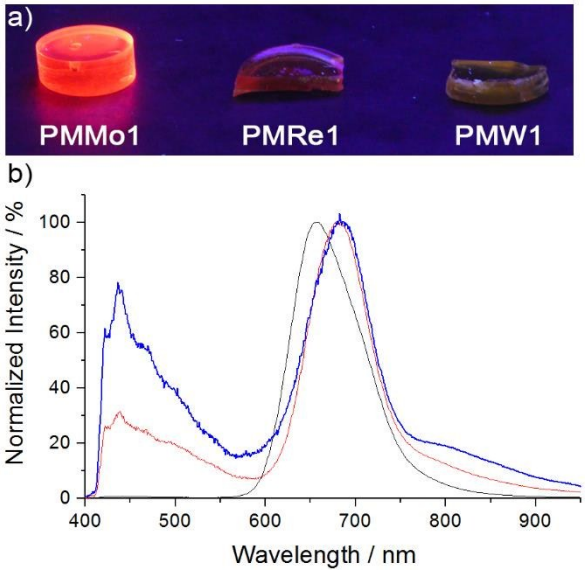

Figure 3. Digital photographs of the pellets a) PMMo1 (left), PMRe1 (middle) and PMW1 (right) under UV (λ_{exc} = 365 nm) and their corresponding emission spectra b) PMMo1 (black line), PMRe1 (red line) and PMW1 (blue line).

Indeed, phosphorescence properties of Mo_6, Re_6 and W_6 clusters are known and well described since the pioneering work of Maverick *et al.*[38] in the early 80's for Mo_6 and W_6 clusters or Yoshimura *et al.*,[39] Guilbaud *et al.*,[40] and Gray *et al.*[41] for Re_6 clusters in 1999. As stated earlier, they all exhibit deep red photoluminescence upon excitation from UV up to 550 nm with phosphorescence lifetimes in the range of several microseconds. Note that we previously demonstrated for the $[Mo_6Br_{14}]^{2-}$ anionic cluster unit that its lifetime was poorly affected when integrated by this ionic technique in PMMA.[32] Thus, qualitatively, the cluster incorporation in the PMMA matrix does not affect its intrinsic luminescence properties. As observed for the parent cluster precursors, the emission maxima of PMRex and PMWx are slightly red shifted of about 30 nm as compared to PMMox samples and, PMWx emission band is slightly wider than the one of PMMox or PMRex. A cautious look at the emission spectra shape reveals the existence of several overlapping emission bands that might correspond, as some of us very recently described for $[Mo_6Br_{14}]^{2-}$ anionic cluster unit, to the simultaneous emission of several excited states.[42] Such cluster behaviour within a polymer matrix will be confirmed in due course.

Spectra of PMRe1 and PMW1 show another emission band centred at 430 nm that corresponds to the emission of the PMMA matrix. Indeed, it has been already observed and reported that PMMA emits weakly in the blue region and that the contribution of this emission depends on the excitation wavelength.[43] We also reported previously that some energy transfer between a PMMA matrix and Re_6 clusters could be expected as the emission band of the PMMA decreased when the content of the Re_6 cluster increased.[11] In this study, we observed the same phenomenon, since the spectra of PMRe20 and PMW50 (ESI figures S13, S14) show that the emission of the PMMA disappears when the cluster amount increases. In the case of PMMo1, the emission of the PMMA matrix cannot be observed as the Mo_6 cluster core is highly emissive. The absolute quantum yields of clusters and their corresponding PMMA hybrids have been studied in the solid state. The results are summarised in **Table 2**.

As expected from the previous works reported by Sokolov *et al*.[19] or Kirakci *et al*.[20] for similar compounds, $Cs_2[Mo_6I_8(C_2F_5COO)_6]$ (**1**) is highly emissive with an absolute emission quantum yield in the solid state of 0.35. This kind of fluorocarboxylated clusters present, indeed, the highest quantum yield value for M_6 clusters complexes. In solution, quantum yields of 0.59 and 1 were reported for $[((n\text{-}C_4H_9)_4N)_2Mo_6I_8(C_3F_7COO_6)]$ and $[((n\text{-}C_4H_9)_4N)_2Mo_6I_8(CF_3COO_6)]$ respectively, whereas in the solid state, a quantum yield value of 0.39 was determined for $[((n\text{-}C_4H_9)_4N)_2Mo_6I_8(C_3F_7COO_6)]$. For the W_6 and Re_6 hybrids the values of ϕ_{em} obtained are 0.05 and 0.07, respectively. These results are in agreement with previously reported works.[11, 18, 31] It has to be noted that intense photoemission for Mo halide clusters units, $[Mo_6X_{14}]^{2-}$, X= Cl, Br, with quantum yields around 0.20 have been reported.[18] The emission properties of the $Cs_2Mo_6I_{14}$ cluster, precursor of (**1**), were studied by Grasset *et al*.[16] who found an emission maximum at 700 nm and that this cluster was not stable and decomposed during experiments. The study of the cluster quantum yield embedded in the PMMA matrix shows that the hybrids containing the Mo_6 cluster (**1**) present the highest ϕ_{em} value as compared to Re_6 or W_6 clusters containing hybrids. The highest ϕ_{em} is found for PMMo1 and PMMo10, 0.27, which is only slightly lower than the ϕ_{em} value of the native cluster (**1**) alone. The ϕ_{em} decreases with the increase of cluster content to 0.20 for PMMo20 and 0.15 for PMMo50.

Table 2. Emission properties of the clusters and the corresponding PMMA hybrids.

Sample	λ_{max}	$\phi_{em\ (solid)}$
$Cs_2[Mo_6I_8(C_2F_5OCO)_6]$ (**1**)	650	0.35
$(H_3O)_2[W_6Cl_{14}]$(**2**)	680	0.05
$K_4[Re_6Se_8(CN)_6]$ (**3**)	685	0.07
PMMo1	650	0.27
PMMo10	650	0.27
PMMo20	650	0.20
PMMo50	650	0.15
PMW1	680	0.04
PMW50	680	0.03
PMRe1	685	0.08
PMRe20	685	0.05

To assess that the luminescent nanocomposite may be suitable for the design of lighting or light conversion devices, photostability studies were realised, by irradiating continuously the samples at λ = 360 nm while recording the luminescence spectra at defined timelaps. **Figure 4** presents results obtained for the PMMox series while **Figure 5** shows the evolution of the phosphorescence intensity of PMRe1 and PMW1 recorded under continuous irradiation.

Surprisingly, the emission intensity increases largely for PMMo samples upon continuous irradiation. This increase, by factors of 1.5 for PMMo1 and 3.5 for PMMo10 and PMMo20, is observed during the first 5 minutes of exposure time; the intensity becomes stable afterwards. On the contrary, the emission intensity of PMMo50 is constant all over the time range. This phenomenon, which is not observed with the native cluster (**1**), is attributed to the low molecular oxygen permeability of the PMMA matrix.

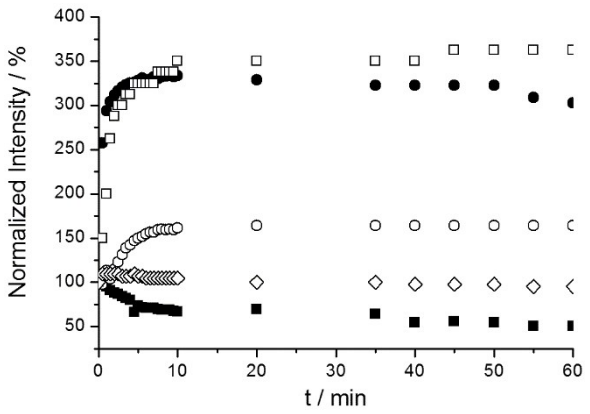

Figure 4. Photostability of Mo_6-PMMA hybrids under UV irradiation for 60 min. (■) compound **1**, (○) PMMo1, (●) PMMo10, (□) PMMo20 and (◊) PMMo50.

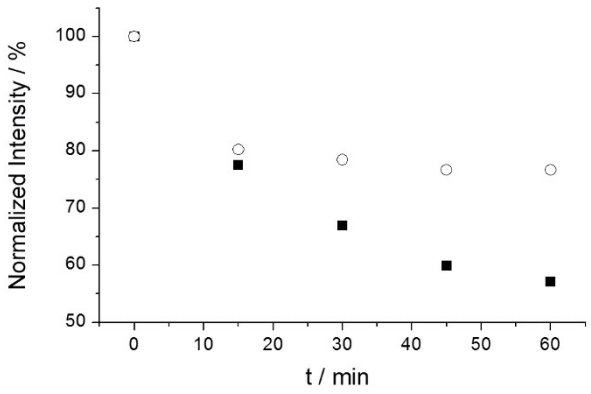

Figure 5. Photostability of Re_6-PMMA and W_6-PMMA hybrids under UV irradiation for 60 min. (○) PMRe1, (■) PMW1.

Very recently, we observed similar phenomena when (**1**) was embedded either in a highly permeable polyurethane matrix or in a liquid crystalline one.[44, 45] Hence, by analogy, we suspect a modification of the clusters local environment within the host matrix. Molecular oxygen, trapped within the copolymer during the synthesis, interacts with metallic clusters that are known to convert it into singlet oxygen (which causes a quenching of the cluster luminescence).[46] After some time under irradiation, when all molecular oxygen is consumed, metallic clusters may be able to enter in a stationary regime and express fully their emitting abilities. Therefore, we can assume that AQY values determined for PMMo1, PMMo10 and PMMo20 are largely underestimated as the irradiation time needed to perform this measurements is in the range of few milliseconds. Thus, considering an increase of the emission intensity of about 3.5 times for PMMo1 and PMMo10, their AQY value, after few minutes of continuous irradiation, should be in the range of 0.7 up to 1 which is in good accordance with literature data.[19, 20, 45] However, although PMMA is not known to be very permeable to O_2, the nanocomposites gas permeability depends highly on their composition and history. Thus, no clear rule between the nanocomposites composition and their gas permeability can be drawn.[47] AQY measurements realised alternatively in an air or a N_2 atmosphere (samples were left 15 min in an integrating sphere saturated with N_2 before AQY acquisition) did not lead, for any of the doped copolymer samples, to significant variation of the AQY values. This, confirms the low permeability to O_2 of all samples. Surprisingly, the photostability studies of PMRe and PMW have shown a completely different behaviour: no enhancement of the luminescence intensity was observed but a decrease by 25 % for PMRe1 and 45 % for PMW1 after one hour of irradiation followed by a stabilisation. One possible explanation of this intensity lowering might be either a photoactivated redox process for PMRe (the reversible oxidation of $[Re_6Se_8(CN)_6]^{4-}$ in $[Re_6Se_8(CN)_6]^{3-}$ occurs at a very low potential, 0.27 V vs SCE, and the metal-CN apical bond is well-known to be one of the most stable in metal cluster chemistry)[48] or a photoinduced apical ligand exchange for PMW samples. We must emphasise at this stage that this is the first time that such behaviour is reported for transition metal cluster containing hybrid compounds and that further investigations, out of the scope of this work, are needed to fully understand this specific photophysical behaviour.

Conclusions

In summary, we show that by integrating polymerisable functions into cationic organic entities we can easily functionalise any type of anionic inorganic nanoclusters and introduce them homogeneously in an organic polymeric matrix. One of the major advantage of this electrostatic approach is to keep intact the anionic metallic core and its inner and apical ligands. In this way, the optical properties of the cluster core remain unchanged in the nanocomposites. Thus, following this general method we have introduced three octahedral anionic cluster building blocks namely, $[Mo_6I_8(C_2F_5COO_6)]^{2-}$, $[Re_6Se_8(CN)_6]^{4-}$ and $[W_6Cl_{14}]^{2-}$ into a PMMA matrix by free-radical polymerisation. As the clusters are held inside the organic matrix by electrostatic interactions, high cluster content, up to 50 wt% for PMMo and PMW and 20 wt% for PMRe, can be incorporated without altering the processability of the polymers. All nanocomposites present deep-red luminescence properties and, in particular, hybrid materials containing $[Mo_6I_8(C_2F_5COO_6)]^{2-}$ are highly emissive showing emission quantum yields that range from 0.15 to 0.27, depending on the cluster amount integrated within the polymer. Interestingly, photostability studies have shown that continuous irradiation of PMMo nanocomposite induces a drastic enhancement of the deep red luminescence intensity making these hybrid materials promising candidates for the development of devices needing strong deep red emitters.

Acknowledgements

This work was financially supported by Fondation Langlois and SATT Ouest-Valorisation. Part of the work was realised in the frame of the French Russian international laboratory CLUSTPOM and ANR Clustomesogen ANR-13-BS07-0003-01. Authors thank Pr. O. Guillou and S. Freslon (TGA), Dr. F. Camerel (DSC) and Dr. J.L. Audic (SEC). Dr. T. Roisnel is acknowledged for crystal structure determination of compound (**1**).

Notes and references

1. E. Holder, N. Tessler and A. L. Rogach, *J. Mater. Chem.*, 2008, **18**, 1064-1078; O. García, R. Sastre, I. García-Moreno, V. Martín and Á. Costela, *Journal of Physical Chemistry C*, 2008, **112**, 14710-14713; X. Li, X. Ni, Z. Liang and Z. Shen, *J. Polym. Sci., Part A: Polym. Chem.*, 2012, **50**, 509-516; S. Kantheti, R. Narayan and K. V. S. N. Raju, *Polym. Int.*, 2015, **64**, 267-274.
2. J.-C. G. Bünzli and S. V. Eliseeva, *J. Rare Earths*, 2010, **28**, 824-842; C. Feldmann, T. Jüstel, C. R. Ronda and P. J. Schmidt, *Adv. Func. Mater.*, 2003, **13**, 511-516; Y. Yuan, F.-S. Riehle, R. Nitschke and M. Krüger, *Mater. Sci. Eng., B*, 2012, **177**, 245-250; C. Zhang and J. Lin, *Chem. Soc. Rev.*, 2012, **41**, 7938-7961.
3. S. Li, M. S. Toprak, Y. S. Jo, J. Dobson, D. K. Kim and M. Muhammed, *Adv. Mater.*, 2007, **19**, 4347-4352; D. Sun, H.-J. Sue and N. Miyatake, *J. Phys. Chem. C*, 2008, **112**, 16002-16010.

4. X. Luo, J. Han, Y. Ning, Z. Lin, H. Zhang and B. Yang, *J. Mater. Chem.*, 2011, **21**, 6569-6575; H. Song and S. Lee, *Nanotechnology*, 2007, **18**, 055402.
5. S. Gross, G. Trimmel, U. Schubert and V. D. Noto, *Polym. Adv. Technol.*, 2002, **13**, 254-259.
6. Y. Han, Y. Xiao, Z. Zhang, B. Liu, P. Zheng, S. He and W. Wang, *Macromolecules*, 2009, **42**, 6543-6548.
7. D. Li, H. Li and L. Wu, *Polym. Chem.*, 2014, **5**, 1930.
8. H. Li, W. Qi, W. Li, H. Sun, W. Bu and L. Wu, *Adv. Mater.*, 2005, **17**, 2688-2692.
9. M. K. Corbierre, N. S. Cameron, M. Sutton, S. G. J. Mochrie, L. B. Lurio, A. Rühm and R. B. Lennox, *J. Am. Chem. Soc.*, 2001, **123**, 10411-10412; A. V. Fuchs and G. D. Will, *Polymer*, 2010, **51**, 2119-2124.
10. M. Amela-Cortes, S. Cordier, N. G. Naumov, C. Mériadec, F. Artzner and Y. Molard, *J. Mater. Chem. C*, 2014, **2**, 9813-9823; A. S. Mocanu, M. Amela-Cortes, Y. Molard, V. Circu and S. Cordier, *Chem. Commun.*, 2011, **47**, 2056-2058.
11. Y. Molard, F. Dorson, V. Cîrcu, T. Roisnel, F. Artzner and S. Cordier, *Angew. Chem. Int. Ed.*, 2010, **49**, 3351-3355.
12. F. Dorson, Y. Molard, S. Cordier, B. Fabre, O. Efremova, D. Rondeau, Y. Mironov, V. Cîrcu, N. Naumov and C. Perrin, *Dalton Trans.*, 2009, 1297-1299.
13. G. Prabusankar, Y. Molard, S. Cordier, S. Golhen, Y. Le Gal, C. Perrin, L. Ouahab, S. Kahlal and J.-F. Halet, *Eur. J. Inorg. Chem.*, 2009, **2009**, 2153-2161; H. D. Selby, B. K. Roland and Z. Zheng, *Acc. Chem. Res.*, 2003, **36**, 933-944.
14. M. A. Shestopalov, S. Cordier, O. Hernandez, Y. Molard, C. Perrin, A. Perrin, V. E. Fedorov and Y. V. Mironov, *Inorg. Chem.*, 2009, **48**, 1482-1489.
15. S. Ababou-Girard, S. Cordier, B. Fabre, Y. Molard and C. Perrin, *ChemPhysChem*, 2007, **8**, 2086-2090; T. Aubert, F. Grasset, S. Mornet, E. Duguet, O. Cador, S. Cordier, Y. Molard, V. Demange, M. Mortier and H. Haneda, *J. Colloid Interface Sci.*, 2010, **341**, 201-208; D. Dybtsev, C. Serre, B. Schmitz, B. Panella, M. Hirscher, M. Latroche, P. L. Llewellyn, S. Cordier, Y. Molard, M. Haouas, F. Taulelle and G. r. Férey, *Langmuir*, 2010, **26**, 11283-11290; B. Fabre, S. Cordier, Y. Molard, C. Perrin, S. Ababou-Girard and C. Godet, *J. Phys. Chem. C*, 2009, **113**, 17437-17446.
16. F. Grasset, F. Dorson, S. Cordier, Y. Molard, C. Perrin, A.-M. Marie, T. Sasaki, H. Haneda, Y. Bando and M. Mortier, *Adv. Mater.*, 2008, **20**, 143-148.
17. T. G. Gray, C. M. Rudzinski, E. E. Meyer, R. H. Holm and D. G. Nocera, *J. Am. Chem. Soc.*, 2003, **125**, 4755-4770; T. G. Gray, C. M. Rudzinski, D. G. Nocera and R. H. Holm, *Inorg. Chem.*, 1999, **38**, 5932-5933; N. Kitamura, Y. Ueda, S. Ishizaka, K. Yamada, M. Aniya and Y. Sasaki, *Inorg. Chem.*, 2005, **44**, 6308-6313.
18. A. W. Maverick, J. S. Najdzionek, D. MacKenzie, D. G. Nocera and H. B. Gray, *J. Am. Chem. Soc.*, 1983, **105**, 1878-1882.
19. M. N. Sokolov, M. A. Mihailov, E. V. Peresypkina, K. A. Brylev, N. Kitamura and V. P. Fedin, *Dalton Trans.*, 2011, **40**, 6375-6377.
20. K. Kirakci, P. Kubát, M. Dušek, K. Fejfarová, V. Šícha, J. Mosinger and K. Lang, *Eur. J. Inorg. Chem.*, 2012, 3107-3111.
21. S. Gross, V. Di Noto and U. Schubert, *J. Non-Cryst. Solids*, 2003, **322**, 154-159; B. Moraru, N. Hüsing, G. Kickelbick, U. Schubert, P. Fratzl and H. Peterlik, *Chem. Mater.*, 2002, **14**, 2732-2740.
22. K. Kirakci, S. Cordier and C. Perrin, *Z. Anorg. Allg. Chem.*, 2005, **631**, 411-416.
23. J. R. Long, L. S. McCarty and R. H. Holm, *J. Am. Chem. Soc.*, 1996, **118**, 4603-4616.
24. J. H. Golden, H. Deng, F. J. DiSalvo, J. M. J. Fréchet and P. M. Thompson, *Science*, 1995, **268**, 1463-1466.
25. O. A. Adamenko, G. V. Loukova and V. A. Smirnov, *Russ. Chem. Bull.*, 2002, **51**, 994-997; O. A. Adamenko, G. V. Lukova, N. D. Golubeva, V. A. Smirnov, G. N. Boiko, A. D. Pomogailo and I. E. Uflyand, *Dokl. Phys. Chem.*, 2001, **381**, 275-278.
26. L. M. Robinson and D. F. Shriver, *J. Coord. Chem.*, 1996, **37**, 119-129.
27. Y. Molard, C. Labbé, J. Cardin and S. Cordier, *Adv. Func. Mater.*, 2013, **23**, 4821-4825.
28. B. K. Roland, W. H. Flora, M. D. Carducci, N. R. Armstrong and Z. Zheng, *J. Cluster Sci.*, 2003, **14**, 449-458.
29. X. Tu, G. S. Nichol, P. Keng, J. Pyun and Z. Zheng, *Macromolecules*, 2012, **45**, 2614-2618.
30. Y. Molard, F. Dorson, K. A. Brylev, M. A. Shestopalov, Y. Le Gal, S. Cordier, Y. V. Mironov, N. Kitamura and C. Perrin, *Chem. Eur. J.*, 2010, **16**, 5613-5619.
31. O. A. Efremova, K. A. Brylev, O. Kozlova, M. S. White, M. A. Shestopalov, N. Kitamura, Y. V. Mironov, S. Bauer and A. J. Sutherland, *J. Mater. Chem. C*, 2014, **2**, 8630-8638.
32. M. Amela-Cortes, A. Garreau, S. Cordier, E. Faulques, J.-L. Duvail and Y. Molard, *J. Mater. Chem. C*, 2014, **2**, 1545-1552.
33. V. Kalyani, V. S. V. Satyanarayana, S. V., C. P. P., S. Ghosh, S. K. Sharma and K. E. Gonsalves, *Chem. Eur. J.*, 2015, **21**, 2250.
34. H. Li, P. Li, Y. Yang, W. Qi, H. Sun and L. Wu, *Macromol. Rapid Commun.*, 2008, **29**, 431.
35. V. Kolesnichenko and L. Messerle, *Inorg. Chem.*, 1998, **37**, 3660-3663.
36. N. G. Naumov, A. V. Virovets, N. V. Podberezskaya and V. E. Fedorov, *J. Struct. Chem.*, 1997, **38**, 857-862.
37. T. Aubert, A. Y. Ledneva, F. Grasset, K. Kimoto, N. G. Naumov, Y. Molard, N. Saito, H. Haneda and S. Cordier, *Langmuir*, 2010, **26**, 18512-18518.
38. A. W. Maverick, J. S. Najdzionek, D. MacKenzie, D. G. Nocera and H. B. Gray, *J. Am. Chem. Soc.*, 1983, **105**, 1878-1882; A. W. Maverick and H. B. Gray, *J. Am. Chem. Soc.*, 1981, **103**, 1298-1300.
39. T. Yoshimura, S. Ishizaka, K. Umakoshi, Y. Sasaki, H. B. Kim and N. Kitamura, *Chem. Letters*, 1999, 697-698.
40. C. Guilbaud, A. Deluzet, B. Domercq, P. Molinie, C. Coulon, K. Boubekeur and P. Batail, *Chem. Commun.*, 1999, 1867-1868.
41. T. G. Gray, C. M. Rudzinski, D. G. Nocera and R. H. Holm, *Inorg. Chem.*, 1999, **38**, 5932-5933.
42. K. Costuas, A. Garreau, A. Bulou, B. Fontaine, J. Cuny, R. Gautier, M. Mortier, Y. Molard, J.-L. Duvail, E. Faulques and S. Cordier, *Phys. Chem. Chem. Phys.*, 2015, DOI: 10.1039/C5CP03960F.
43. R. S. Fonseca, M. Flores, R. Rodriguez, J. Hernandez and A. Munoz, *J. Lum.*, 2001, **93**, 327-332.
44. S. M. Wood, M. Prévôt, M. Amela-Cortes, S. Cordier, S. J. Elston, Y. Molard and S. M. Morris, *Adv. Optical Mater.*, 2015, DOI: 10.1002/adom.201500257.
45. M. Prevot, M. Amela-Cortes, S. K. Manna, R. Lefort, S. Cordier, H. Folliot, L. Dupont and Y. Molard, *Adv. Func. Mater.*, 2015, **25**, 4966-4975; M. Amela-Cortes, S. Paofai, S. Cordier, H. Folliot and Y. Molard, *Chem. Commun.*, 2015, **51**, 8177-8180.
46. J. A. Jackson, C. Turro, M. D. Newsham and D. G. Nocera, *J. Phys. Chem.*, 1990, **94**, 4500-4507.
47. S. Hess, A. Becker, S. Baluschev, V. Yakutkin and G. Wegner, *Macromol. Chem. Phys.*, 2007, **208**, 2173-2188; S. Hess, M. M. Demir, V. Yakutkin, S. Baluschev and G. Wegner, *Macromol. Rapid Commun.*, 2009, **30**, 394-401.
48. M. Amela-Cortes, S. Cordier, N. G. Naumov, C. Meriadec, F. Artzner and Y. Molard, *J. Mater. Chem. C*, 2014, **2**, 9813-9823.

Versatility of the Ionic Assembling Method to Design Highly Luminescent PMMA Nanocomposites Containing $[M_6Q^i_8L^a_6]^{n-}$ Octahedral Nano-building Blocks

M. Amela-Cortes, Y. Molard, S. Paofai, A. Desert, J.-L. Duvail, N. G. Naumov, S. Cordier

Strongly luminescent hybrids nanocomposites were designed by integrating via an ionic technique high content of different transition metal clusters.